

CrystEngComm

Accepted Manuscript



This is an *Accepted Manuscript*, which has been through the Royal Society of Chemistry peer review process and has been accepted for publication.

Accepted Manuscripts are published online shortly after acceptance, before technical editing, formatting and proof reading. Using this free service, authors can make their results available to the community, in citable form, before we publish the edited article. We will replace this *Accepted Manuscript* with the edited and formatted *Advance Article* as soon as it is available.

You can find more information about *Accepted Manuscripts* in the [Information for Authors](#).

Please note that technical editing may introduce minor changes to the text and/or graphics, which may alter content. The journal's standard [Terms & Conditions](#) and the [Ethical guidelines](#) still apply. In no event shall the Royal Society of Chemistry be held responsible for any errors or omissions in this *Accepted Manuscript* or any consequences arising from the use of any information it contains.

COMMUNICATION

A rare case of a dye co-crystal showing better dyeing performance

Cite this: DOI: 10.1039/x0xx00000x

Hui-Fen Qian,^{a,b} Yin-Ge Wang,^b Jiao Geng,^a and Wei Huang^{*a}Received,
Accepted

DOI: 10.1039/x0xx00000x

www.rsc.org/

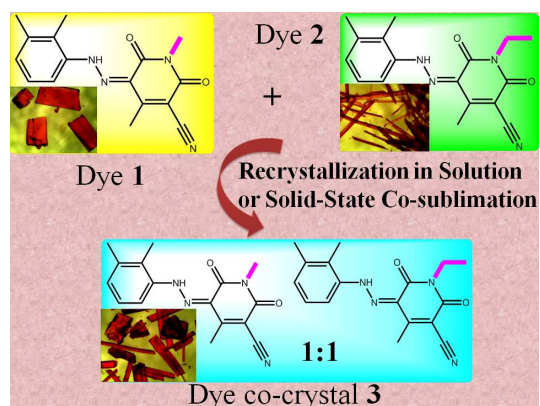
A rare case of a pyridine-2,4-dione based heterocyclic dye co-crystal, composed of a 1:1 molar ratio of two structural analogs (pyridine *N*-Me and *N*-Et substituents) in the hydrazone form, is described with better dyeing performance, and this dye co-crystal can be prepared by both recrystallization in solution and solid-state co-sublimation methods.

Co-crystal structures are a special family of compounds exhibiting long-range order, and the components interact via non-covalent interactions. They can generate physical and chemical properties that differ from the properties of the individual components.¹ Nowadays co-crystals have found applications in a number of fields such as active pharmaceutical ingredients (API),² nonlinear optical³ and energetic materials.⁴ In addition, investigations on the co-crystals and related compounds have become part of a highlight on crystal growth and crystal engineering in the past decade.⁵

In dyestuff industry, an empirical and low-risk strategy in the process of dyeing is using a dye composition having similar molecular structures to improve their dyeing behavior such as dispersion stability, tinting strength, built-up property, and washing and sublimation fastness. However, the possible reason and dyeing mechanism are still not well-known because the dyeing process is very complicated and many factors may influence the final dyeing performance. Furthermore, successful characterization of single-crystal structures of dye co-crystals is still very challenging, because the most likely outcome is the appearance of two separate molecular solids when a homogeneous solution containing two different solutes is allowed to evaporate to grow single-crystals.

Pyridine-2,4-dione based heterocyclic dyes are one of important aromatic heterocycle azo dyes, and they have shown brilliant color, high chromophoric strength and excellent light fastness.⁶ In our previous work, a series of pyridine-2,4-dione, quinoline-2,4-dione and 1*H*-pyrazol-3-one based disperse yellow dyes crystallizing in the hydrazone form in the solid state and their azo-hydrazone tautomerisms driven by pH titration and metal-ion complexation have been investigated.⁷ In this report, a rare case of a dye co-crystal **3** composed of a 1:1 molar ratio of two structural analogs (**1** and **2**) in the hydrazone form is described (Scheme 1), where both of **1** and

2 are pyridine-2,4-dione based heterocyclic dyes having different *N*-substituted groups (*N*-Me in **1** and *N*-Et in **2**). It is found that the dye co-crystal can be prepared by both recrystallization in solution and solid-state co-sublimation methods and it exhibits better dyeing performance than its individual components.



Scheme 1. Molecular structures of dyes **1-3** together with their single-crystal photos.

Dyes **1** and **2** can be easily prepared by classical diazotization and the following coupling reactions in satisfactory yields. The two dyes have the same diazonium component (2,3-dimethylaniline) but different coupling components (1,4-dimethyl-3-cyano-6-hydroxypyrid-2-one in **1** and 3-cyano-4-methyl-6-hydroxy-*N*-ethyl-2-pyridone in **2**). There are two methods to prepare co-crystal dye **3**. One follows the same method of **1** and **2** but only a mixture of half molar amounts of 1,4-dimethyl-3-cyano-6-hydroxypyrid-2-one and 3-cyano-4-methyl-6-hydroxy-*N*-ethyl-2-pyridone is used. The resultant mixture undergoes the following solid-state co-sublimation under reduced pressure. The other is just mixing equal molar ratio of dyes **1** and **2** and undergoing the following solid-state co-sublimation.

As can be seen in Fig. S11-3, the FT-IR spectra of dyes **1-3** displayed characteristic absorption bands at 1632, 1623, and 1632 cm^{-1} assigned as the stretching vibrations of common hydrazone unit.

In addition, typical absorption peaks are observed at 2220, 2225, and 2227 cm^{-1} in dyes **1-3** corresponding to the stretching vibrations of C \equiv N group. The molecular ion peak of three compounds [M-H]⁻ can be clearly observed in their negative ESI-TOF-MS spectra, as depicted in Fig. SI4-6. UV-vis spectra of dyes **1-3** having the same benzene/pyridine-2,6-dione skeleton have been recorded in their methanol solutions with the same concentration of $3.0 \times 10^{-5} \text{ mol} \cdot \text{L}^{-1}$, as can be seen in Fig. SI7. There are two similar absorption peaks for three dyes centered at 268 and 443 nm ($\zeta = 13833$ and $39733 \text{ L} \cdot \text{cm}^{-1} \cdot \text{mol}^{-1}$) in **1**, 268 and 442 nm ($\zeta = 15267$ and $41500 \text{ L} \cdot \text{cm}^{-1} \cdot \text{mol}^{-1}$) in **2**, and 269 and 444 nm ($\zeta = 15333$ and $54933 \text{ L} \cdot \text{cm}^{-1} \cdot \text{mol}^{-1}$) in **3**, which are ascribed to the $n-\pi^*$ transitions between the phenyl rings and the middle hydrazone units and the $\pi-\pi^*$ transitions within the whole molecules, respectively.

In their ¹H NMR spectra (Fig. SI8-SI10), all data confirmed the expected structures of heterocyclic azo dyes and the assignments of different protons can be easily done by means of the deshielding effects and the split of peaks. The chemical shifts (δ) of the hydrazone proton in compounds **1-3** are located at 15.33-15.36 ppm, and the hydrogen atoms of benzene rings in the range of 7.13-7.67 ppm. In addition, a singlet at $\delta = 3.40$ ppm was observed for dye **1** corresponding to three N-CH₃ protons, and two peaks are found at 4.07 and 1.26 ppm for dye **2** corresponding to five N-Et protons. In contrast, dye **3** has three peaks at 4.10, 3.42 and 1.29 ppm simultaneously assigned as three N-CH₃ and five N-Et protons. The ratio of 2:3:3 obtained from the peak integration demonstrates that the dye co-crystal is composed of a 1:1 molar ratio of two structural analogs **1** and **2**. That is to say, the dye co-crystal is a pure compound before it is dissolved in the organic solvent.

It is noted that dyes **1-3** have different growing habit of the single-crystals, as shown in Scheme 1. Namely, dye **1** tends to form block-like single crystals, while dye **2** is apt to form needle-like ones. In contrast, co-crystal dye **3** has both block-like and needle-like crystalline forms, which can be verified by X-ray single-crystal diffraction studies. The melting point of dye **3** is decreased to 228–230 °C in comparison with its two individual components (264–266 °C for dye **1** and 244–246 °C for dye **2**), also indicating the character of a pure compound. It is suggested that the decrease of melting point for co-crystal dye **3** favors forming more stable and uniform colloidal suspension owing to the effective decrease of the lattice energy.

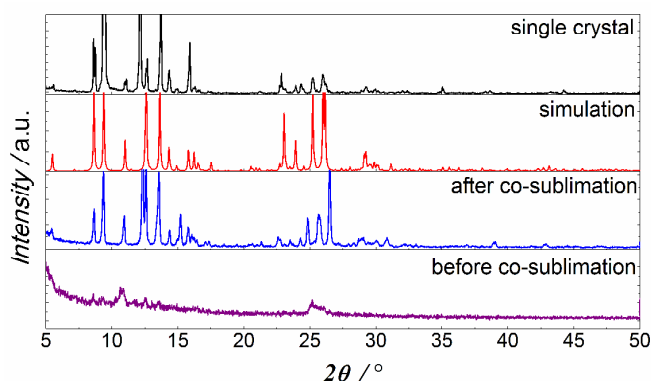


Fig. 1. Simulative (red line) and experimental PXRD patterns (black line) of dye co-crystal **3**, together with those of equal molar amounts of **1** and **2** mixture before (purple line) and after (blue line) co-sublimation.

It is interesting to mention that dye co-crystal **3** can be easily prepared by both recrystallization in chloroform and solid-state co-sublimation under reduced pressure with high yields (70–80 %). As shown in Fig. 1, the pure phase of dye **3** is confirmed by the powder

X-ray diffraction (PXRD) pattern after recrystallization in chloroform (black line), where the experimental curves are in good agreement with the simulative one (red line) obtained from its single-crystal structure. More importantly, a physical mixture of equal molar amounts of **1** and **2**, which were obtained directly from the diazotization and the following coupling reactions, shows very poor phase purity before co-sublimation (purple line), but the PXRD pattern becomes much better after solid-state co-sublimation (blue line), indicating the possibility of large scale production and further application of this co-crystal in dye industry.

Thermogravimetric analysis and differential scanning calorimetry (TGA–DSC) are two commonly used methods in order to determine melting points, phase transitions, and enthalpic factors which can be compared to each individual cocrystal former. As can be seen in Fig. SI11, the TGA–DSC diagram of dye **1** reveals that it has no weight loss until 270 °C, and after that it begins to decompose with a sharp exothermic DSC peak at 273 °C. However, there is a melting process evidenced by an endothermic DSC peak at 268 °C. In comparison with dye **1**, the TGA–DSC curve of dye **2** (Fig. SI12) indicates that it has no weight loss until 250 °C, and after that it starts to decompose with a sharp exothermic DSC peak at 265 °C. Also, there is a melting process for dye **2**, which is evidenced by an endothermic DSC peak at 245 °C. In contrast, dye **3** has no weight loss until 240 °C (Fig. SI13), and it starts to decompose with an exothermic DSC peak at 260 °C. There is a melting process, too, which is evidenced by an endothermic DSC peak at 230 °C. The thermal properties of dyes **1-3** demonstrate the slight decrease of melting point and decomposition temperature of co-crystal dye **3** in comparison with its two individual components.

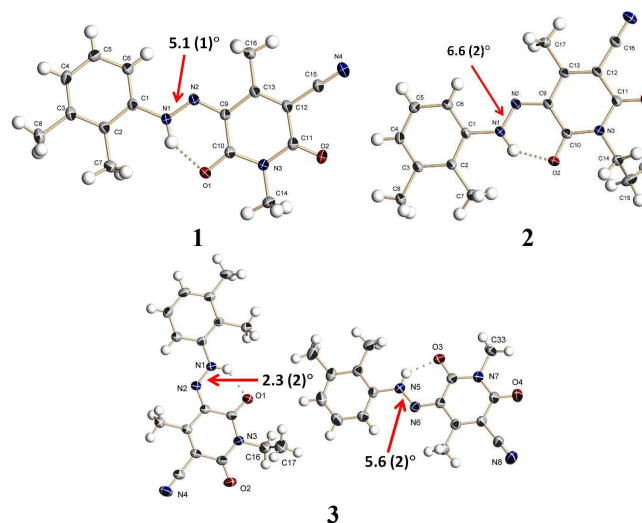


Fig. 2. ORTEP diagrams (30% thermal probability ellipsoids) of the molecular structures of dyes **1**, **2**, and **3** showing the dihedral angles between adjacent aromatic heterocycles.

The molecular structures of dyes **1** and **2** with the atom-numbering scheme are shown in Fig. 2a and Fig. 2b, respectively. X-ray structural analyses⁸ reveal that both **1** and **2** crystallize in the same triclinic $P\bar{1}$ space group and no solvent molecules are present in their unit cells. The dihedral angles between the two aromatic rings in dyes **1** and **2** are 5.1(1) and 6.6(2)°, respectively, indicative of good planarity of the whole molecules. Moreover, intramolecular N–H \cdots O hydrogen bonding interactions are observed in each of them (Table SI3), forming similar six-membered hydrogen bonded rings and further stabilizing the whole planar molecular structures.

Although the term “co-crystal” is believed to be “*scientifically suspect*” by Desiraju⁹ and “*not perfect*” by Dunitz¹⁰ because there is still controversy on its definition up till now especially on the inclusion or exclusion of salts, clathrates, hydrates and solvates (polymorphs or pseudopolymorphs).¹¹ Dye **3** is indeed a co-crystal by any standard. Different from **1** and **2**, dye **3** has a distinguishable unit cell and two sets of crystallographically independent molecules are present. The dihedral angle between their molecular least-squares planes is calculated to be 19.3(2)°. The dihedral angles between the two aromatic rings in each molecule are 2.3(2) and 5.6(2)°, respectively, also exhibiting good planarity of the whole molecules (Fig. 2c). In addition, analogous six-membered intramolecular hydrogen bonded rings are observed in each of molecules in dye co-crystal **3**.

The high quality of single-crystal diffraction data of dyes **1-3** makes possible the precise localization of every hydrazone proton. Furthermore, the related N–N, C–N, and C–C bond lengths indicate clearly the formation of hydrazone tautomers for dyes **1-3**. These are believed to be a powerful crystallographic proof to verify the formation of hydrazone tautomers for dyes **1-3**. In the crystal packing, both **1** and **2** show the same AAAA packing mode without any π - π stacking interactions. In contrast, dye co-crystal **3** displays a different packing fashion where its two components (shown as red and yellow molecules) are stacked individually and arranged alternately, as displayed in Fig. 3.

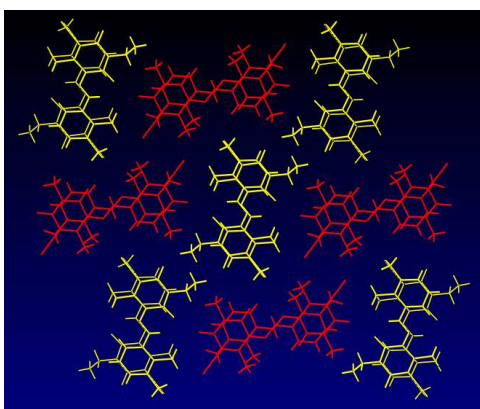


Fig. 3. Crystal packing view of co-crystal dye **3** where two components are shown as red (dye **1**) and yellow (dye **2**), respectively.

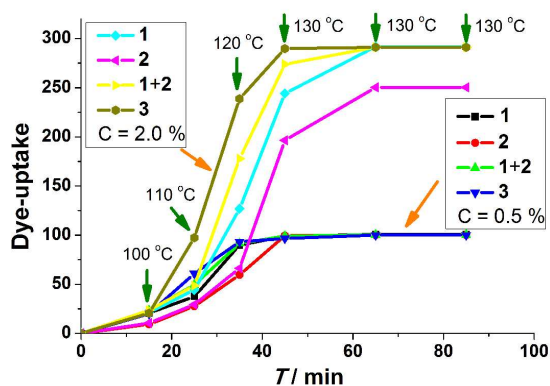


Fig. 4. Dyeing rate curves for disperse yellow dyes **1**, **2**, **1+2** mixture with equal molar ratio, and **3** with OWF % as 0.5 and 2.0 %, respectively. Dye-uptake of disperse yellow dye **2** at 130 °C for 40 minutes was set as 100%.

Considering that dye co-crystal **3** may have different dyeing performance from its individual components, which is originated

from their distinguishable intermolecular interactions and resulting crystal structures. Determination of dye-uptake for disperse yellow dyes **1**, **2**, mixture of equal molar amounts of **1** and **2**, and **3** at high temperature dyeing on acrylic fibers has been carried out with the percentage of weight of fabric (OWF %) as 0.5 and 2.0 %, respectively, together with C.I. Disperse Red 60 and C.I. Disperse Blue 56 for comparison (Fig. 4 and Table S12). The results reveal that **2** has lower dye-uptake in comparison with **1** especially in a higher OWF % value, indicative of relatively poor build-up of *N*-Et dye. However, this weak point can be improved by using a physical mixture of **1** and **2**, where the two dye synonyms show good compatibility with each other. It is noted that dye co-crystal **3** exhibits the best performance on the dyeing rate in the temperature range 100–130 °C and it reaches the maximum in the shortest time, which may originate its more stable and uniform colloidal suspension under the same experimental condition. This means that the use of dye co-crystal could have the best dyeing performance with minimum energy consumption. In addition, dye co-crystal **3** demonstrates good match with trichromatic blue and red, especially with C.I. Disperse Red 60, which could make it a good candidate for the trichromatic yellow dye in dyestuff industry.

In summary, a rare case of a dye co-crystal **3** composed of a 1:1 molar ratio of two structural analogs (**1** and **2**) in the hydrazone form is described in this work. The dye co-crystal can be prepared by both recrystallization in solution and solid-state co-sublimation methods. The character of a pure compound for co-crystal dye **3** instead of a mixture has been clearly verified by the melting point, single-crystal structure and powder X-ray diffraction data, ¹H NMR and ESI-TOF-MS spectra, and TGA-DSC analyses. More interestingly, dye co-crystal **3** exhibits the best dye-uptake and built up to fabrics in comparison with its individual components **1** and **2** as well as the dye composition of **1** and **2**. The current study is suggested to throw some new light on the understanding of composite and co-crystal dyes.

This work was financially supported by the Major State Basic Research Development Programs (Nos. 2013CB922101 and 2011CB933300), the National Natural Science Foundation of China (No. 21171088), and the Natural Science Foundation of Jiangsu Province (Grant BK20130054).

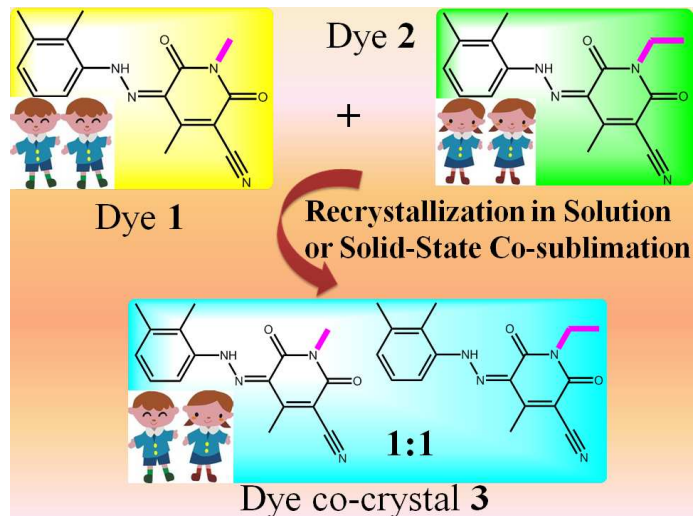
Notes and references

^a State Key Laboratory of Coordination Chemistry, Nanjing National Laboratory of Microstructures, School of Chemistry and Chemical Engineering, Nanjing University, Nanjing 210093, P. R. China; E-mail: whuang@nju.edu.cn; ^b College of Sciences, Nanjing Tech University, Nanjing, Jiangsu Province, 210009, P. R. China

† Electronic Supplementary Information (ESI) available: Syntheses of dyes **1-3**. Tables for crystallographic data and standard determination of dye-uptake. Figures for FT-IR, ESI-MS, UV-Vis, ¹H NMR, and TGA-DSC spectra. CCDC 1034365-1034367. For crystallographic data in CIF or other electronic format See DOI:10.1039/b000000x/

- (a) D. Braga, F. Grepioni, L. Maini and M. Polito, *Struct. Bond*, 2009, **132**, 25; (b) M. J. Zaworotko, *Cryst. Growth Des.*, 2007, **7**, 4; (c) T. Rager and R. Hilfiker, *Cryst. Growth Des.*, 2010, **10**, 3237.
- (a) M. C. Etter, *J. Phys. Chem.*, 1991, **95**, 4601; (b) P. Vishweshwar, J. A. McMahon, J. A. Bis and M. J. Zaworotko, *J. Pharm. Sci.*, 2006, **95**, 499; (c) N. Blagden, D. J. Berry, A. Parkin, H. Javed, A. Ibrahim, P. T. Gavan, L. L. De Matos and C. C. Seaton, *New J. Chem.*, 2008, **32**, 1659; (d) Y. Yan, J. M. Chen, N. Geng and T. B. Lu, *Cryst. Growth Des.*, 2012, **12**, 2226; (e) Q. Tao, J. M. Chen, L. Ma and T. B. Lu, *Cryst. Growth Des.*, 2012, **12**, 3144; (f) Y. Yan, J. M. Chen and T. B. Lu, *CrystEngComm*, 2013, **15**, 6457; (g) B. S. Sekhon, *ARS Pharm.*, 2009, **50**, 99; (h) A. V. Trask, *Mol. Pharm.*, 2007, **4**, 301.

- 3 (a) F. Pan, M. S. Wong, V. Gramlich, C. Bosshard and P. Günter, *J. Am. Chem. Soc.*, 1996, **118**, 6315; (b) M. S. Wong, F. Pan, M. Bösch, R. Spreiter, C. Bosshard, P. Günter and V. Gramlich, *J. Opt. Soc. Am. B*, 1998, **15**, 426.
- 4 O. Bolton, L. R. Simke, P. F. Pagoria and A. J. Matzger, *Cryst. Growth Des.*, 2012, **12**, 4311.
- 5 (a) S. Aitipamula, R. Banerjee, A. K. Bansal, K. Biradha, M. L. Cheney, A. R. Houdhury, G. R. Desiraju, A. G. Dikundwar, R. Dubey, N. Duggirala, P. P. Ghogale, S. Ghosh, P. K. Goswami, N. R. Goud, R. K. R. Jetti, P. Karpinski, P. Kaushik, D. Kumar, V. Kumar, B. Moulton, A. Mukherjee, G. Mukherjee, A. S. Myerson, V. Puri, A. Ramanan, T. Rajamannar, C. M. Reddy, N. Rodriguez-Hornedo, R. D. Rogers, T. N. G. Row, P. Sanphui, N. Shan, G. Shete, A. Singh, C. C. Sun, J. A. Swift, R. Thaimattam, T. S. Thakur, R. K. Thaper, S. P. Thomas, S. Tothadi, V. R. Vangala, N. Variankaval, P. Vishweshwar, D. R. Weyna and M. J. Zaworotko, *Cryst. Growth Des.*, 2012, **12**, 2147; (b) M. J. Zaworotko, *Cryst. Growth Des.*, 2007, **7**, 4; (c) C. B. Aakeröy and D. J. Salmon, *CrystEngComm*, 2005, **7**, 439; (d) A. D. Bond, *CrystEngComm*, 2007, **9**, 833.
- 6 (a) A. D. Towns, *Dyes Pigm.*, 1999, **42**, 3; (b) K. Hunger, *Industrial dyes: chemistry, properties, applications*, 3rd ed. Weinheim: Wiley-VCH; 2003; (c) H. Zollinger, *Color chemistry: synthesis, properties and application of organic dyes and pigments*, 3rd ed. Zürich: Wiley-VCH; 2003.
- 7 (a) W. Huang, *Dyes Pigm.*, 2008, **79**, 69; (b) W. You, H. Y. Zhu, W. Huang, B. Hu, Y. Fan and X. Z. You, *Dalton Trans.*, 2010, **39**, 7876; (c) X. C. Chen, T. Tao, Y. G. Wang, Y. X. Peng, W. Huang and H. F. Qian, *Dalton Trans.*, 2012, **41**, 11107; (d) X. C. Chen, Y. G. Wang, T. Tao, J. Geng, W. Huang and H. F. Qian, *Dalton Trans.*, 2013, **42**, 7679; (e) H. F. Qian, Y. G. Wang, Y. Dai, J. Geng, W. G. Ruan and W. Huang, *Dyes Pigm.*, 2015, **112**, 67.
- 8 X-ray crystallographic data for dye **1**: C₁₆H₁₆N₄O₂, *M* = 296.33, *T* = 291(2) K, triclinic, space group, *P* $\bar{1}$, *a* = 7.399(1) Å, *b* = 7.516(1) Å, *c* = 13.583(1) Å, α = 100.737(1)°, β = 93.491(1)°, γ = 103.171(1)°, *V* = 718.32(8) Å³, *Z* = 2, μ = 0.094 mm⁻¹, *D_c* = 1.370 g·cm⁻³, *F*(000) = 312, reflections collected / independent, 4062 / 2501, refinement method, full-matrix least-squares on *F*², parameters, 207, *S* = 1.07, *R*₁ [*I* > 2σ(*I*)] = 0.0437, *wR*₂ (all data) = 0.1384. Residual electron density, 0.19 / -0.20 e·Å⁻³. Dye **2**: C₁₇H₁₈N₄O₂, *M* = 310.35, *T* = 291(2) K, triclinic, space group, *P* $\bar{1}$, *a* = 8.072(1) Å, *b* = 9.924(1) Å, *c* = 11.132(1) Å, α = 65.872(1)°, β = 80.149(2)°, γ = 74.023(2)°, *V* = 780.60(16) Å³, *Z* = 2, μ = 0.090 mm⁻¹, *D_c* = 1.320 g·cm⁻³, *F*(000) = 328, reflections collected / independent, 5679 / 2699, refinement method, full-matrix least-squares on *F*², parameters, 216, *S* = 1.09, *R*₁ [*I* > 2σ(*I*)] = 0.0575, *wR*₂ (all data) = 0.1754. Residual electron density, 0.23 / -0.34 e·Å⁻³. Dye **3**: C₃₃H₃₄N₈O₄, *M* = 606.68, *T* = 291(2) K, triclinic, space group, *P* $\bar{1}$, *a* = 7.811(2) Å, *b* = 12.550(4) Å, *c* = 16.146(5) Å, α = 94.579(5)°, β = 91.539(5)°, γ = 98.774(5)°, *V* = 1558.0(8) Å³, *Z* = 2, μ = 0.088 mm⁻¹, *D_c* = 1.293 g·cm⁻³, *F*(000) = 640, reflections collected / independent, 8747 / 5458, refinement method, full-matrix least-squares on *F*², parameters, 421, *S* = 0.90, *R*₁ [*I* > 2σ(*I*)] = 0.0645, *wR*₂ (all data) = 0.1986. Residual electron density, 0.56 / -0.32 e·Å⁻³.
- 9 G. R. Desiraju, *CrystEngComm*, 2003, **5**, 466.
- 10 J. D. Dunitz, *CrystEngComm*, 2003, **5**, 506.
- 11 (a) K. R. Seddon, *Cryst. Growth Des.*, 2004, **4**, 1087; (b) J. Bernstein, *Cryst. Growth Des.*, 2005, **5**, 1661; (c) A. Nangia, *Cryst. Growth Des.*, 2006, **6**, 2.

A rare case of a dye co-crystal showing better dyeing performance**Hui-Fen Qian, Yin-Ge Wang, Jiao Geng, Wei Huang,***

A rare case of a dye co-crystal composed of a 1:1 molar ratio of two structural analogs is described showing better dyeing performance, and the dye co-crystal can be prepared by both recrystallization in solution and solid-state co-sublimation methods.

